

# A Regional Surface Wave Magnitude Scale for the Earthquakes of Russia's Far East

O. S. Chubarova<sup>a, \*</sup> and A. A. Gusev<sup>a, b, \*\*</sup>

<sup>a</sup>*Institute of Volcanology and Seismology, Russian Academy of Sciences, bulv. Piip 9, Petropavlovsk-Kamchatskii, 683006 Russia*

<sup>b</sup>*Kamchatka Branch, Geophysical Survey, Russian Academy of Sciences, bulv. Piip 9, Petropavlovsk-Kamchatskii, 683006 Russia*

\*e-mail: ochubarova@emsd.ru

\*\*e-mail: gusev@emsd.ru

Received June 4, 2015

**Abstract**—The modified scale  $M_s(20R)$  is developed for the magnitude classification of the earthquakes of Russia's Far East based on the surface wave amplitudes at regional distances. It extends the applicability of the classical Gutenberg scale  $M_s(20)$  towards small epicentral distances ( $0.7^\circ$ – $20^\circ$ ). The magnitude is determined from the amplitude of the signal that is preliminarily bandpassed to extract the components with periods close to 20 s. The amplitude is measured either for the surface waves or, at fairly short distances of  $0.7^\circ$ – $3^\circ$ , for the inseparable wave group of the surface and shear waves. The main difference of the  $M_s(20R)$  scale with the traditional  $M_s(BB)$  Soloviev–Vanek scale is its firm spectral anchoring. This approach practically eliminated the problem of the significant (up to  $-0.5$ ) regional and station anomalies characteristic of the  $M_s(BB)$  scale in the conditions of the Far East. The absence of significant station and regional anomalies, as well as the strict spectral anchoring, make the  $M_s(20R)$  scale advantageous when used for prompt decision making in tsunami warnings for the coasts of Russia's Far East.

**Keywords:** earthquake, magnitude scale, surface waves, Soloviev, Gutenberg, bandpass filter

**DOI:** 10.1134/S1069351316060021

## INTRODUCTION

Many versions of the magnitude classification of the earthquakes have been developed to date. Each of them provides the quantitative characteristic of the earthquake in terms of the power of its source as a source of elastic waves. The first magnitude scale suggested by Richter in 1935 was regional; Gutenberg extended it to the teleseismic distances. Gutenberg discovered the high efficiency of the maximum amplitudes  $A$  of the surface wave group with periods  $T$  of about 20 s for these purposes and, based on this, constructed the global scale  $M_s^{(Gut)}(20)$  applicable in the interval of the epicentral distances from  $20^\circ$  to  $180^\circ$ . I. Vanek and S.L. Soloviev suggested using the maximum of the  $A/T$  ratio instead of  $A$ , which extended the range of the epicentral distance to  $2^\circ$ – $180^\circ$  and enabled magnitude determination for many earthquakes at regional distances from the waves with shorter periods (as short as 3 s).

Simultaneously, this approach bypassed the problem associated with the fact that the common instrument of the Soviet seismic networks, SK, with a pendulum period of 10–12 s, was not quite acceptable for identifying and picking up waves with periods of about

20 s. Vanek and Soloviev have somewhat changed the Gutenberg's magnitude calibration function and obtained the known Prague formula (Vanek et al., 1962). The Vanek–Soloviev scale, referred to as  $M_s(BB)$  in the present-day nomenclature, is the standard in the world and Russian seismology (Bormann et al., 2002; 2007); it was employed in the former Soviet Union since its creation. At the same time, the leading American seismic service—NEIC (USA)—has not accepted this standard.

Following Gutenberg (1945), NEIC only uses the maximum amplitudes within a given, not very wide range of the apparent periods of 18–22 s and only for distances above  $20^\circ$ . For obtaining such a spectrally definite magnitude scale in the frequency band of about 0.05 Hz (at periods of about 20 s), NEIC makes use of the dispersion of the surface waves. In NEIC's approach, the attenuation of amplitudes with distance is assumed to follow the Prague formula. The result of this procedure has received the international designation  $M_s(20)$ . The scales  $M_s(20)$  and  $M_s(BB)$  are mutually consistent. We note that the Soloviev–Vanek calibration function was developed for the horizontal components; however, nowadays, it is considered as

universal and is used for the vertical components (Rayleigh waves).

An important limitation of the scales  $M_s^{(Gut)}(20)$  and  $M_s(20)$  is imposed by their inapplicability at small epicentral distances (below  $20^\circ$ ). In this range, the dispersion effects are not yet sufficiently manifest to ensure easy identification of a wave train with a period of  $\sim 20$  s. Meanwhile the magnitude estimates for short distances are essential, particularly due to the fact that this magnitude is used as a basis in a vitally important practical application associated with decision making in the tsunami warning systems. The  $M_s(\text{BB})$  scale manages this problem. The  $M_s(\text{BB})$  scale, the main one in the Russian seismic service, employs the maximum apparent amplitude of the Rayleigh surface waves at the epicentral distances starting from  $2^\circ$ .

This scale relies on the actual observed apparent period of the surface waves which is typically 3–5 s at the short epicentral distances of  $2^\circ$ – $3^\circ$ . With the increase in distance, the apparent period reaches 10–20 s and more. At the distances of  $20^\circ$ , the magnitudes on the  $M_s(20)$  and  $M_s(\text{BB})$  scales are typically close to each other, which almost straightforwardly follows from the similarity of the magnitude scale construction techniques. The typical agreement between the  $M_s(\text{BB})$  estimates between the nearby and remote stations is driven by a different mechanism, i.e., due to the empirical fact of the consistency of the estimates based on the values of the  $A/T$  ratio at different  $T$ , and implicitly relies upon a certain typical structure of the source spectrum. However, the cases of inconsistency originating from the spectral peculiarities of a particular source are also fairly common.

The key limitations of the  $M_s(\text{BB})$  scale are associated with (1) the lack of strict spectral anchoring, which leads to inconveniences for a number of important applications such as estimation of the potential of the devastating tsunami waves and the strong ground motion analysis; (2) the difficulty of accurately measuring the apparent period and picking the amplitude at the small epicentral distances when one has to use a short wave train which is in addition barely separable from the group of the shear waves; and (3) the presence of significant station and regional anomalies.

The problem of spectral anchoring is critical when the magnitude data are used for timely decision making in tsunami warnings for the coasts of Russia's Far East. For announcing a tsunami warning, it is in principle desirable to rely on as-low-as-possible frequencies. From this standpoint, the  $M_s(\text{BB})$  scale is as of now far from optimal, at the same time, it should be recognized that in the predigital era, the solution of Soloviev was reasonable and adequate. The problem of measuring the amplitudes of a fairly broadband signal and the frequently embarrassing visual suppression of the noise also needed to be solved. Finally, the problem of the regional and station anomalies of the

$M_s(\text{BB})$  scale is particularly acute in the conditions of Russia's Far East where these anomalies reach  $-0.5$  (Solov'ev, 1974).

Attempts were made to improve the situation by introducing the system of regional and stationary corrections; however, no clear solution was obtained. In (Chebrov et al., 2013), the authors analyzed the time behavior of the residual of the magnitude  $M_s(\text{BB})$  at the Petropavlovsk seismic station relative to the network's average magnitude during the period from 1967 to 2007 and showed that this residual was not only not small but, besides, varied significantly under the changes in the recording system and data processing procedure. The limitations of the commonly accepted magnitude scales based on the surface waves were previously noted in (Evernden, 1971; Marshall and Basham, 1973; von Seggern, 1977; Panza et al., 1989; Herak, M. and Herak, D., 1993; Rezapour and Pearce, 1998; Alewine, 1972; Okal, 1989), and various solutions were suggested for improving the calibration curves.

These problems necessitated the development of a new regional modification of the  $M_s$  scale. The present paper addresses this task. Our idea consists in using a digital filter for selecting the components of the signal in the vicinity of the period of 20 s at small distances where a natural selection of these oscillations through dispersion does not work. The new modification is hereinafter denoted by  $M_s(20R)$ . A similar approach to the creation of the regional magnitude scale was applied in (Singh and Pacheco, 1994), where the authors used the period range between 15 and 30 s.

The first stage of constructing the  $M_s(20R)$  scale is described in (Chubarova et al., 2011). The present paper presents the further steps in the suggested approach and includes the refined version of the calibration functions, which is the key new achievement of our study.

## INITIAL DATA

As the initial data for this work, we used the records of 433 Northwestern Pacific earthquakes of 1993–2009 by 12 broadband digital seismic stations (PET, YSS, MA2, YAK, KAM, ADK, TIXI, BILL, MDJ, INCN, ERM, and MAJO), totaling 1659 three-component records of the BH channel. The digital records of the earthquakes were selected from the IRIS DMC data archive (<http://www.iris.edu/dMs/wilber.htm>) and the tsunami database of the Kamchatka Branch of the Geophysical Survey of the Russian Academy of Sciences (KB GS RAS). The depths of the earthquake sources are up to 70 km. Only the earthquakes for which the estimates of teleseismic magnitudes  $M_s(20)$  were contained in the NEIC catalog (<http://neic.usgs.gov/neis/epic/epic.html>) were selected. The magnitudes of the selected earthquakes range from 4.0 to 8.2. The initial digital records were processed by the DIMAS software

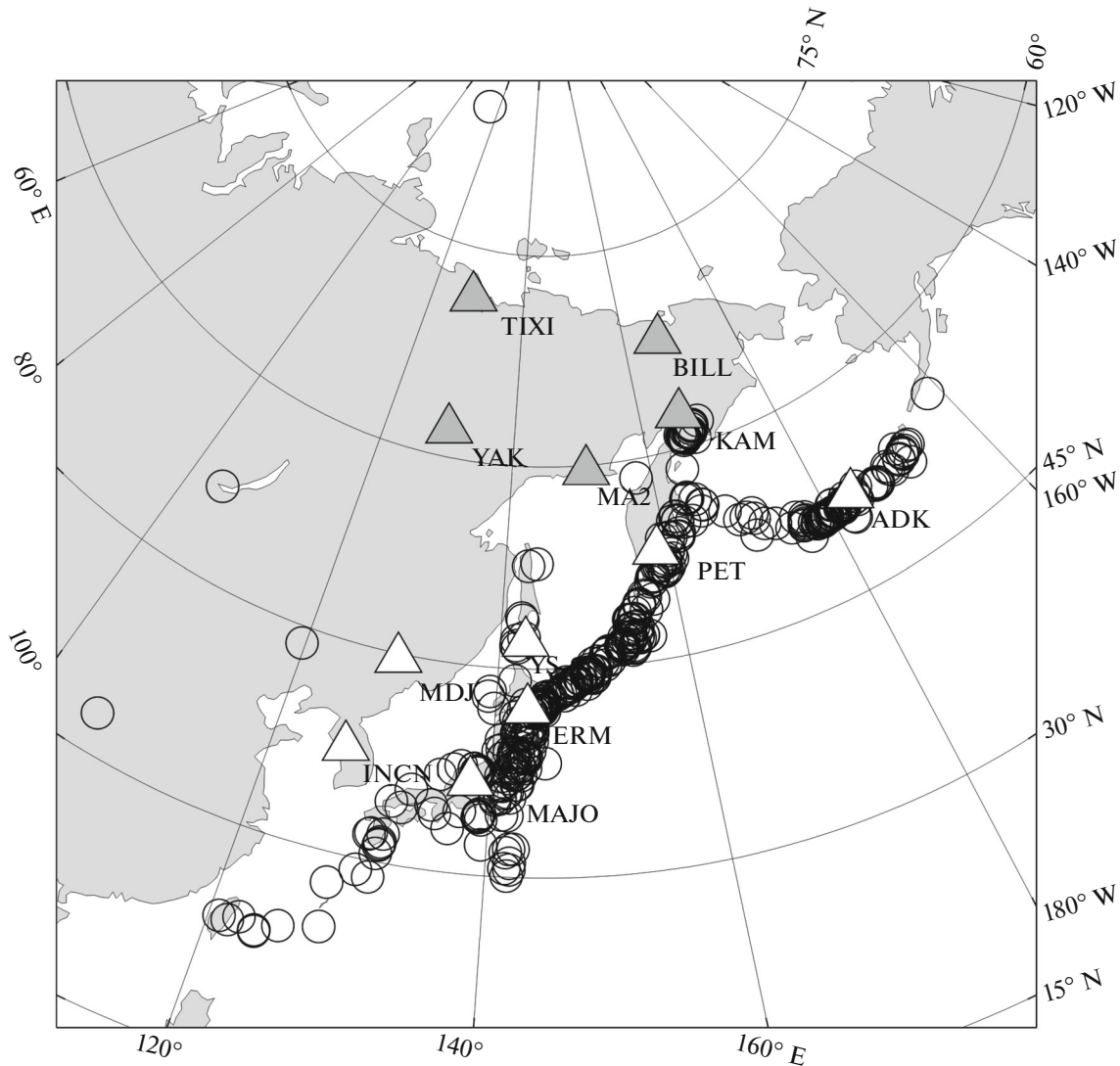


**Fig. 1.** The epicentral map of the Northwestern Pacific earthquakes (the circles) with the layout of the digital seismic stations (the triangles) used for constructing the calibration functions. The stations are subdivided into two classes—the island-arc stations (white filled) and continental stations (gray filled), each class with its own calibration function.

developed by D.V. Droznin (KB GS RAS) (Droznin and Droznina, 2011).

The layout of the seismic stations and the epicenters of the processed earthquakes are shown in Fig. 1.

#### THE PROCEDURE FOR DETERMINING THE AMPLITUDES

For constructing the calibration functions, we examined the distance dependence of the maximum amplitudes of the surface wave displacements subjected to bandpass filtering with a central frequency of 0.05 Hz. We employed the physically implementable (causal) fourth-order Butterworth filter with the cutoff frequencies of 0.0625 and 0.04 Hz (periods 16–25 s). The filter was applied to the displacement signal

obtained by inverse filtering the velocity signal of BH channel. The observed amplitude  $A_{\text{obs}}$  was normalized to the expected amplitude  $A_{20^\circ}$  of a given earthquake at the reference epicentral distance  $\Delta = 20^\circ$ , calculated by the Prague formula from the value of the teleseismic magnitude value  $M_s(20)$  of this event presented in the NEIC catalog.

The peak amplitudes were measured within a time window with a length of 600 s starting from the arrival of the  $S$ -wave ( $[t_s, t_s + 600 \text{ s}]$ , where  $t_s$  is the  $S$ -wave arrival time). The maximum values in each of the three components were picked at independent time instants (the example of the record of the earthquake and the conducted measurements is presented in Fig. 2). To control which waves' maxima are measured, we examined the dependence between the time  $t_L$  (counted from the

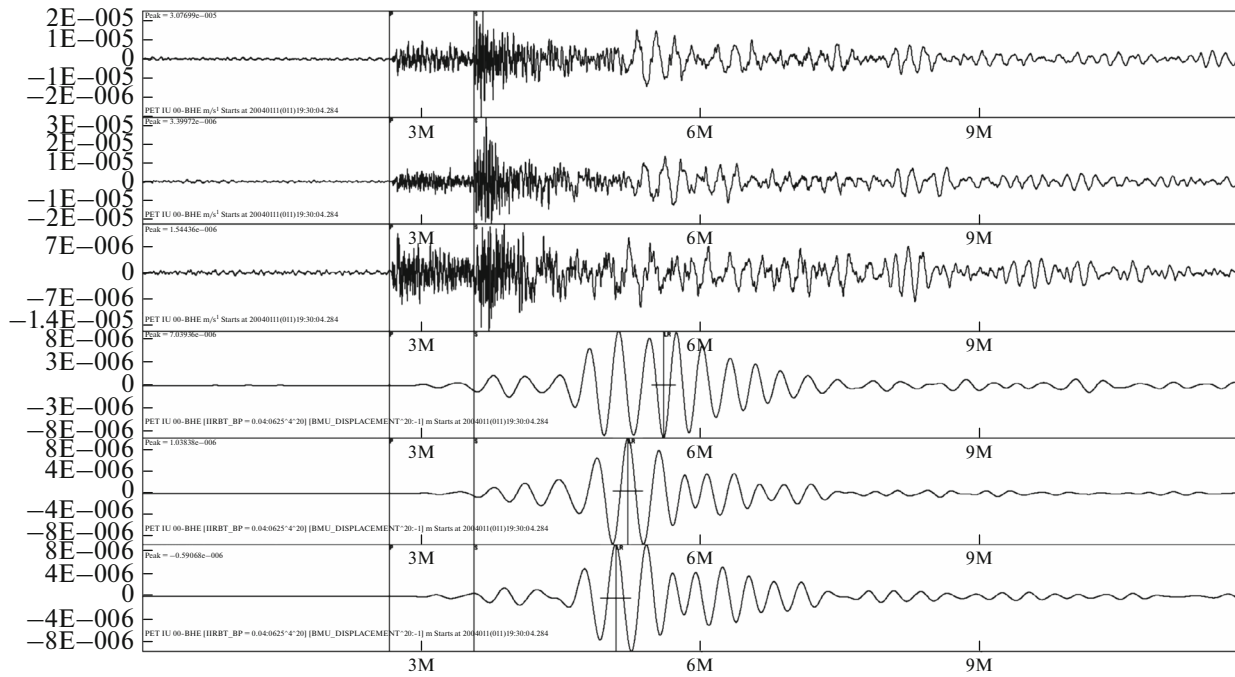


**Fig. 2.** The example of the record of the earthquake and the conducted measurements (the screenshot of the dialog box of the DIMAS program). The top three traces are the velocigraph signal components BHE, BHN, and BHZ. The three bottom traces show the results of bandpass filtering of the ground displacement signal. The time step (along the abscissa axis) is 3 min. The vertical lines mark the *P*- and *S*-wave arrivals and the time of picking the amplitudes of the filtered surface waves.

origin time) of the picked peak amplitude and the epicentral distance  $\Delta$ . Remarkably, due to the phase shift in the bandpass filter, the measured time  $t_L$  is apparent and is delayed relative to the ideal by about 1.5 periods (the time delay is  $dt_f = 30$  s).

The obtained graphs  $t_L(\Delta)$  are presented in Fig. 3. It can be seen that with the conditionally selected velocities of 2.95 km/s for the vertical component (Rayleigh wave) and 3.15 km/s (Love wave) for the earlier one of the horizontal components, the time instants  $t_L$  are fairly predictable. (The calculated travel times of the Rayleigh and Love surface waves are delayed by  $dt_f$ .) The times  $t_s$  are also indicated in the graphs. It can be seen that the peaks of the filtered surface wave mainly arrive within  $\pm 15\%$  of the calculated arrival time of the waves with the assumed velocities.

For calculating the magnitude for a particular station, it was required to find a way to generalize the measurements of the components. The following options were tested: (1) two amplitudes (and then two magnitudes): one from the vertical component and another from the root mean square (rms) value of the two horizontal components; (2) one amplitude (and then one magnitude) from the average logarithm of the three components; (3), the same, from the rms value of the three components. The corresponding graphs are presented in (Chubarova et al., 2011). It was found that a systematic bias between the amplitudes from the vertical and horizontal components is absent

(Fig. 4). Therefore, it can be believed that a combination of the data from three component amplitudes is quite admissible. The most stable results were obtained in the mode with the rms value of three components; in what follows, we use this option. The same option of combining the component data is selected in (Singh and Pacheco, 1994).

### CONSTRUCTION OF THE CALIBRATION FUNCTION

The accepted common approach to construct the calibration functions of the magnitude scale  $M_s(20R)$  is given below. For an individual earthquake, the known teleseismic estimate of its magnitude  $M_s = M_s(20)_{NEIC}$  from the NEIC catalog is assumed to be the “true” magnitude of this event. The theoretically expected amplitude  $A_{20^\circ}$  of the surface seismic wave from this earthquake at an epicentral distance of  $20^\circ$  is calculated by the Prague formula:

$$\log_{10} A_{20^\circ} = M_s(20)_{NEIC} - 3.3 - 1.66 \log_{10} 20^\circ - \log_{10}(T) \quad (1)$$

at fixed  $T = 20$  s. The value  $A_{20^\circ}$  is subsequently used for reducing (normalizing) the observed amplitude  $A_{obs}$  of the seismic surface wave. The reduced amplitude is

$$A_r = A_{obs} / A_{20^\circ}.$$

The procedure for determining  $A_{obs}$  is described above. It is thought that normalization, on average,

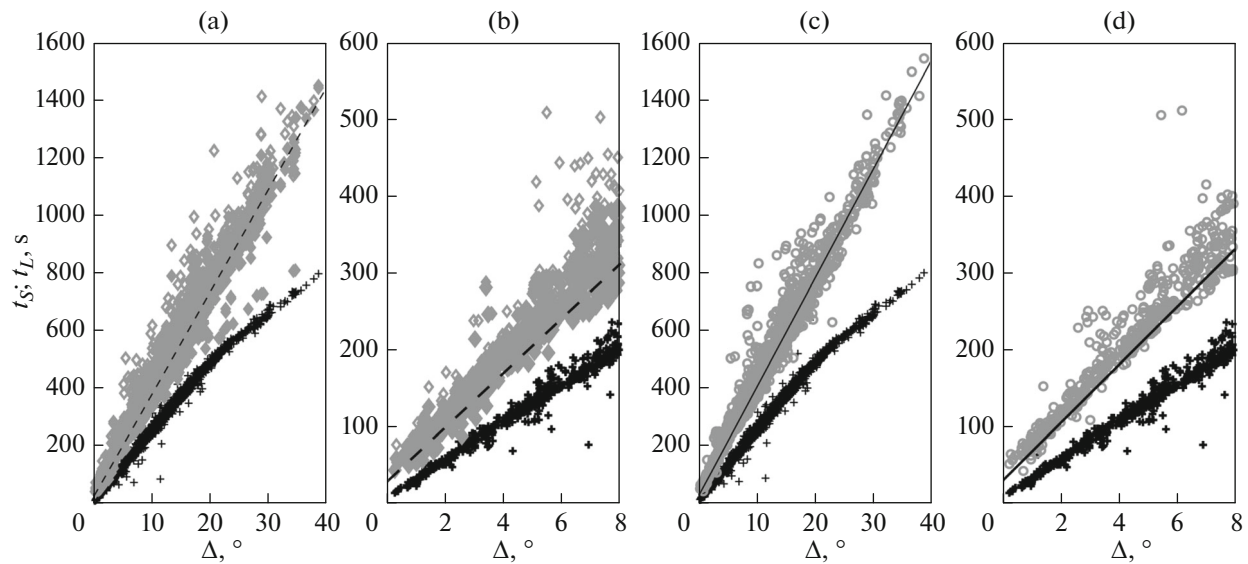


**Fig. 3.** The time  $t_L$  of measuring the displacement amplitude as a function of  $\Delta$  for (a), (b) horizontal and (c), (d) vertical components. Time is measured from  $t_0$ . Graphs (a) and (c) for the total range of times and distances; graphs (b) and (d) for the shorter epicentral distances only. The straight lines are the calculated travel-time curves for the Rayleigh wave with the velocity of 2.95 km/s (the solid line) and for the Love wave with the velocity of 3.15 km/s (the dashed line), incremented by  $dt_f = 30$  s to account for the phase shift in the filter; the diamonds show two horizontal components with a filled marker for the earlier maximum; the circles show the vertical component; the crosses mark the arrivals of the  $S$ -waves picked from the record.

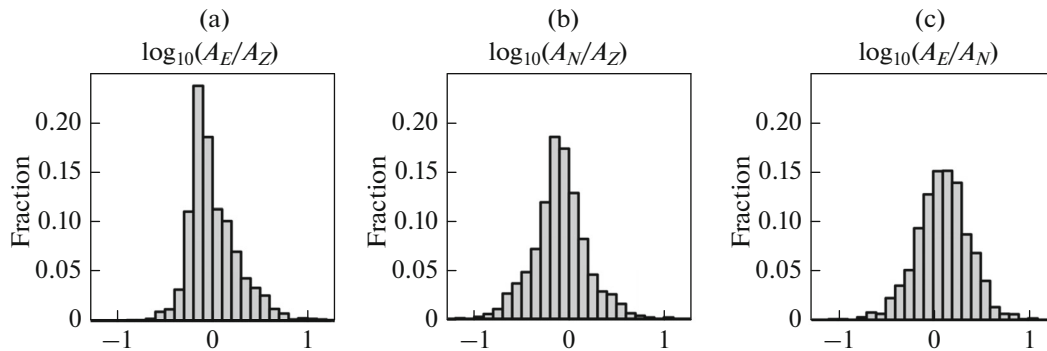


**Fig. 4.** The normalized histograms of logarithmic ratios of the components: (a), for the components  $E$  and  $Z$ , mean 0.01, standard deviation 0.26; (b), for the components  $N$  and  $Z$ , mean  $-0.1$ , standard deviation 0.28; (c), for the components  $E$  and  $N$ , mean 0.1, standard deviation 0.26.

removes the influence of the spectral level of a particular earthquake. Each value  $A_r$  obtained at a particular epicentral distance  $\Delta$  gives one experimental point (estimate) of the dependence of the logarithmic amplitude on distance, i.e., the function

$$a(\Delta) = \log_{10}(A_r(\Delta)).$$

It is implied that the data analysis is conducted based on the record of a certain earthquake by a certain seismic station of the Far Eastern network, which has the epicentral distance  $\Delta$ . From the set of estimates  $a(\Delta)$  obtained from the set of the earthquakes and the set of stations, the averaged dependence  $a(\Delta)$  is calculated, i.e., in fact, the sought calibration function (up to a constant shift). However, this procedure needs significant particularization.

The final recommended (2014) version of the  $M_s(20R)$  scale was actually constructed in three stages. It would be perhaps instructive to briefly describe these stages to make clear the choice of the final version. The initial version of the calibration function was constructed under the assumption that the value of  $A_{20^\circ}$  calculated by formula (1), on average, reflects the real level of the amplitudes from this earthquake at a distance of  $20^\circ$ . Under these conditions, the problem was reduced to finding the function  $a(\Delta)$  within a fixed regional interval of epicentral distances up to  $20^\circ$  ( $\sim 2200$  km). In the ideal case, provided that the Prague formula is valid, the observed data  $a(\Delta) = \log_{10}(A_{\text{obs}}/A_{20^\circ})$  should fall in a certain curve which passes through the zero value at the epicentral distance  $\Delta = 20^\circ$ . Considering this initial assumption, we con-

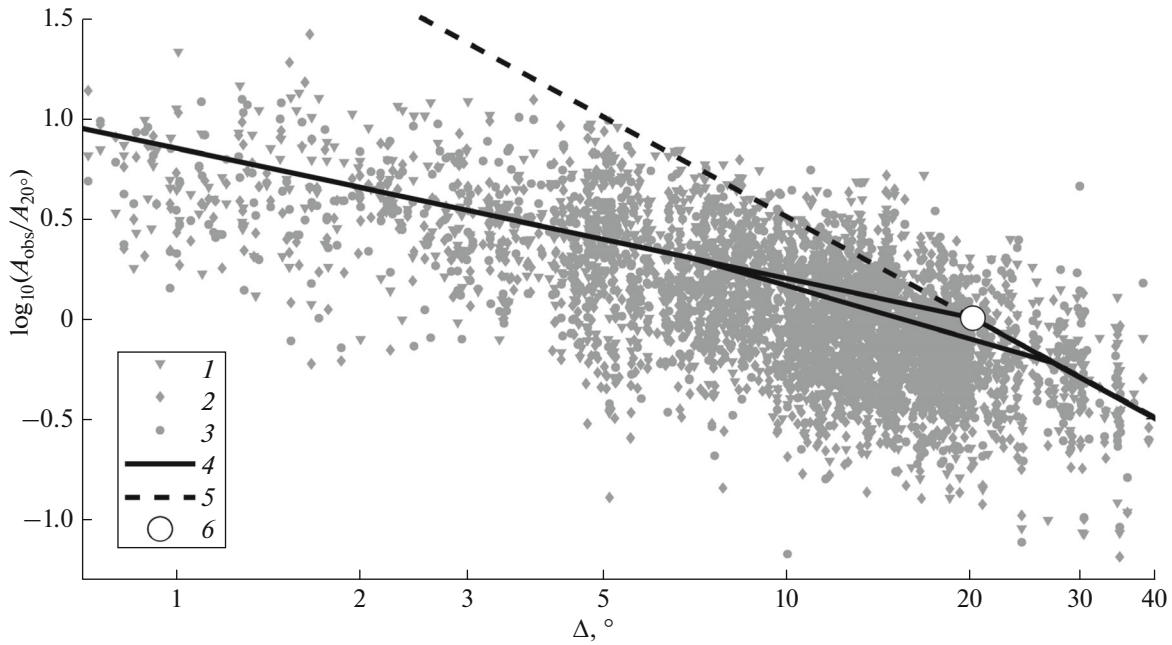


**Fig. 5.** The observed reduced amplitudes  $A_r = A_{\text{obs}}/A_{20^\circ}$  of the components as functions of  $\Delta$ , compared with the first version of the calibration functions. 1, 2, 3, components  $E$ ,  $N$ ,  $Z$ , respectively; 4, the calibration functions in the version of 2009; 5, the calibration functions for the magnitude  $M_s(\text{BB})$ . The latter is only shown for providing a general idea; its difference from the data is expected because the calculation of  $M_s(\text{BB})$  contains the measured apparent period (at  $\Delta < 20^\circ$ , typically  $T = 3\text{--}10$  s) rather than the fixed period  $T = 20$  s; 6, the point of the hypothetical stitching of the regional magnitude scale  $M_s(20\text{R})$  with the teleseismic scale  $M_s(20)$  at the epicentral distance  $\Delta = 20^\circ$ .

structured the average dependence with the additional assumption  $a(\Delta = 20^\circ) = 0$ . This dependence has been constructed and was considered as the initial approximation.

However, this approximation has immediately called for a correction because the empirical values of  $a(\Delta)$  at  $\Delta$  about  $20^\circ$  turned out to be systematically below zero, in obvious contradiction with the ideal picture described above. The analysis guided us to subdivide the stations into two groups with the dissimilar properties. It was found that the deviation from the Prague formula is formed by the data of the main group of stations hereinafter conventionally referred to as the island-arc stations (Fig. 1). At the same time, for the continental stations (Fig. 1), which are located on the periphery of the Eurasian continent, the assumption  $a(\Delta = 20^\circ) = 0$  turned out to be acceptable.

Thus, for the continental stations the Prague formula is valid up to  $\Delta = 20^\circ$ . At the same time, for the island-arc stations, the average  $a(\Delta)$  line at  $\Delta = 20^\circ$  runs below zero (the difference is about  $-0.15$ ). Therefore, in the case of the island-arc stations, in order to avoid the step by 0.15 upwards in the calibration function, we had to extend the new calibration function to the distances above  $20^\circ$ . The new island-arc calibration function was stitched with the Prague formula at  $\Delta = 27^\circ$ . The calibration functions for each group of stations were assumed to be piecewise linear; besides,

they were assumed to be identical over the interval  $\Delta = 2^\circ\text{--}7^\circ$ . The details of constructing this (2009) version of the  $M_s(20\text{R})$  scale and the results of testing it on the data from various seismic stations are presented in (Chubarova et al., 2011).

This stage of the work is illustrated by Fig. 5. Here, the calibration functions—the island-arc (bottom) and continental ones (top), as well as the straight line corresponding to the Prague formula, are shown against the background of the obtained empirical  $a(\Delta)$  data. It is clearly seen that at  $\Delta = 20^\circ\text{--}30^\circ$  the data are definitely below the level expected by the Prague formula.

The new version (2014) of the  $M_s(20\text{R})$  scale was built by revising the initial approach, with the complete rejection of the condition that the new calibration function should be comparable with the Prague formula in the vicinity of  $\Delta = 20^\circ$ . In order to fit the reality, the calibration function of the  $M_s(20\text{R})$  scale was extended up to a distance of  $40^\circ$  (4500 km), and in the interval  $20^\circ\text{--}40^\circ$  it deviates from the Prague formula. Preserving the general approach and adding a certain amount of new data, we updated the calibration function for the island-arc stations. These new functions have a higher degree of detail and never coincide with continental functions at any distance.

We managed to almost completely eliminate the station corrections which have been significantly reduced even in the 2009 scale, compared to the case

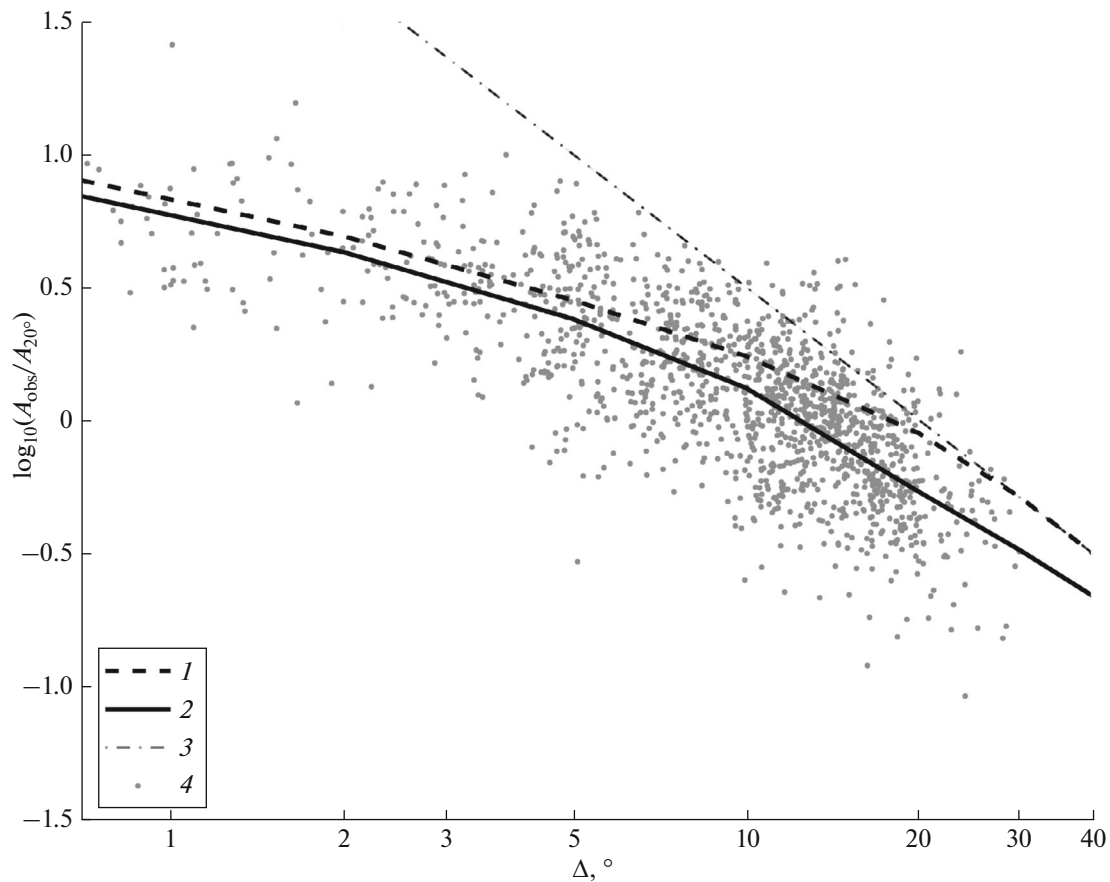


**Fig. 6.** The normalized station amplitudes  $A_r = A_{\text{obs}}/A_{20^\circ}$  and the new calibration functions: 1,  $\tau_1(\Delta)$  for the continental stations; 2,  $\tau_2(\Delta)$  for the island-arc stations; 3, the calibration function by the Prague formula; 4, the observation data obtained from the island-arc stations (the reduced rms value over three components).

of  $M_s(\text{BB})$ , but were still present. However, in one particular case, it was impossible to avoid the correction, as discussed below. For the studied region of Russia's Far East, the new version of the  $M_s(20R)$  scale does not only cover the distance range of interest  $2^\circ$ – $20^\circ$  but may well be recommended for use also in the interval  $\Delta = 20^\circ$ – $40^\circ$  (2200–4500 km) as the refinement of the standard scale  $M_s(20)$ . We note that the numerical changes in the estimates  $M_s(20R)$  associated with the replacement of the calibration function of 2009 (in combination with the corrections) in the calculations by the version of 2014 are fairly small. They are not systematic and in most cases they do not exceed  $\pm 0.1$ .

The selected amplitudes in the form of the station values  $\log_{10}A_r$  for the island-arc stations are drawn in Fig. 6. Based on these data and similar graphs for the continental stations, we constructed the piecewise approximations which are presently recommended as the calibration functions. The location of the two types of stations is shown in Fig. 1.

#### THE RECOMMENDED CALIBRATION CURVES FOR DETERMINING THE MAGNITUDE $M_s(20R)$ AND THE PROCEDURE FOR THEIR USE

The magnitude  $M_s(20R)$  in the current (2014) version is defined by the following formula:

$$\begin{aligned} M_s(20R) &= \log_{10}(A/T) + \sigma(\Delta) \\ &\equiv \log_{10}(A/T) - \tau(\Delta) + 5.460, \end{aligned} \quad (2)$$

where  $\sigma(\Delta)$  is the calibration function in the traditional form;  $\tau(\Delta)$  is its modification which is numerically determined by the algorithm described below;  $\Delta$  is the epicentral distance in degrees,  $0.7^\circ \leq \Delta \leq 40^\circ$ ;  $A$  is the root mean square (over three channels) value of the peak ground displacement amplitude at the output of the digital filter in  $\mu\text{m}$ , within the time window  $[t_s, t_s + 600 \text{ s}]$ ;  $t_s$  is the arrival time of the  $S$ -wave; and  $T$  is the wave period fixed at  $T = 20 \text{ s}$ . In the work with the digital records, instead of  $(A/T)$ , we use  $V_{\text{max}}/2\pi$ , where  $V_{\text{max}}$  is the maximum amplitude of the velocity signal. It is admissible and recommended to determine  $V_{\text{max}}$  as half the double amplitude (peak-to-peak span of the record). The maximum amplitude in the

**Table 1.** The values of the parameters of the calibration functions for the Far Eastern regional surface-wave magnitude scale  $M_s(20R)$  for the set of the nodal points of epicentral distances

Parameters	Epicentral distance $\Delta$ , degree							
	$<0.7^{[1]}$	0.7	2	5	10	20	30	$40^{[2]}$
$\log_{10}(\Delta)$	—	−0.1549	0.3010	0.6990	1.0000	1.3010	1.4771	1.6021
$\tau_1(\Delta)^{[3]}$	—	0.90	0.69	0.45	0.24	−0.05	−0.29	−0.50
$\tau_2(\Delta)^{[4]}$	—	0.84	0.63	0.38	0.12	−0.27	−0.49	−0.66

For the intermediate values of  $\Delta$ , one should use the linear interpolation with respect to the argument  $\log_{10}(\Delta)$ ; <sup>1</sup> at  $\Delta < 0.7^\circ$ , the calibration function is not defined and the magnitude  $M_s(20R)$  cannot be calculated; <sup>2</sup> at  $\Delta = 30^\circ\text{--}40^\circ$ , the calibration function  $\tau_1(\Delta)$  coincides with the Prague formula. <sup>3</sup> For the continental stations; <sup>4</sup> for the island-arc stations.

selected time window either corresponds to the surface wave or, typically at  $\Delta \leq 3^\circ$ , to the inseparable group of the shear and surface waves.

The recommended function  $\tau(\Delta)$  is constructed in two modifications, each intended for one of the two groups of seismic stations:

(1) The stations located at a distance from the marginal seas of the Pacific, for brevity conditionally referred to as continental stations. This type of stations includes the KAM, TIXI, BILL, and YAK stations, their calibration function is denoted by  $\tau_1(\Delta)$ ;

(2) The stations located within the NE Pacific and its margins, including the Mudanjan (MDJ) and Magadan (MA2) stations, for brevity conditionally referred to as island-arc stations. The set of the studied stations of this type includes PET, ADK, MA2, YSS, MDJ, INCN, ERM, and MAJO; their calibration function is denoted by  $\tau_2(\Delta)$ .

The calibration functions are specified by their nodal values for the set of the nodes  $\Delta$  of Table 1. Their values are calculated by the linear interpolation with respect to the argument  $\log_{10}(\Delta)$ . It is worth noting that the calibration function  $\tau_2(\Delta)$  in the interval  $20^\circ\text{--}40^\circ$  is not determined entirely reliably and should be used with caution (see below). At  $\Delta > 40^\circ$  (4500 km), one should, in any case, use the standard calibration function of the  $M_s(20)$  scale (the Prague formula).

At the junction of the new scale with the  $M_s(20)$  scale, certain difficulties arose which need discussion. In Table 1 (see also Fig. 6), the values of  $\tau_1(\Delta)$  are stitched with the Prague formula at  $\Delta = 25^\circ\text{--}40^\circ$  and, in fact, they replicate this formula. At the same time, the values of  $\tau_2(\Delta)$  even at  $\Delta = 40^\circ$  continue deviating downwards from the Prague formula by 0.16. This discrepancy formally means that the subset of the Far Eastern island-arc stations as a whole group has anomalous behavior in terms of the standard (not the new regional) magnitude classification  $M_s(20)$ . This fact is of certain interest and, in principle, it deserves study.

At the same time, it should be borne in mind that the cited results reflect the limited statistics of the existing data, whose selection did not anticipate the

necessity of studying the magnitude scales over such large distances. Nevertheless, the obtained result raises little doubt in the interval  $\Delta = 20^\circ\text{--}30^\circ$  and, hence, the new calibration curves can well be used for the Far Eastern stations even in this interval of the epicentral distances. For the interval  $\Delta = 30^\circ\text{--}40^\circ$ , the suggested recommendations should be considered as tentative until refined on the basis of representative data.

#### CHECKING THE INTERNAL CONSISTENCY OF THE SCALE

For controlling the quality of the magnitude estimated on the new scale, we considered the residuals of the station estimates of the magnitude  $\Delta M_{stN} = M_s(20R) - M_s(20)_{NEIC}$ . Figure 7 illustrates the dependence of the residuals  $\Delta M_{stN}$  on distance and magnitude  $M_s(20)$  and shows the corresponding histogram. It can be seen that the use of the different calibration curves for the island-arc and continental stations resulted in the removal of the significant systematic deviations in the entire considered interval of epicentral distances and entire range of magnitudes.

Besides the residuals  $\Delta M_{stN}$ , it is also interesting to examine the within-network scatter of the station estimates of the new magnitude  $M_s(20R)$  relative to their own mean  $M_s(20R)_R$  over the Far Eastern network, i.e., the residuals  $\Delta M_{st} = M_s(20R)_{st} - M_s(20R)_R$ . Table 2 presents the parameters of the distribution  $\Delta M_{st}$  for each station. The residuals have a standard deviation of 0.18–0.27, which characterizes the internal accuracy of the individual station estimates by the new magnitude classification. This accuracy is typical of such cases. The average residuals of the stations are within  $\pm 0.08$ . Hereinafter, the standard deviations were always calculated with the correction  $(n/(n - 1))^{0.5}$  in order to take into account the small sample size.

Therefore, we have calculated the composite (total by the stations) characteristics of the residuals  $\Delta M_{st}$ , (within-network) and  $\Delta M_{stN}$  (relative to  $M_s(20)_{NEIC}$ ). Besides, we determined the residuals of the network's average magnitude  $M_s(20R)_R$  relative to the magnitude  $M_s(20)_{NEIC}$  (between-network), which we denote by

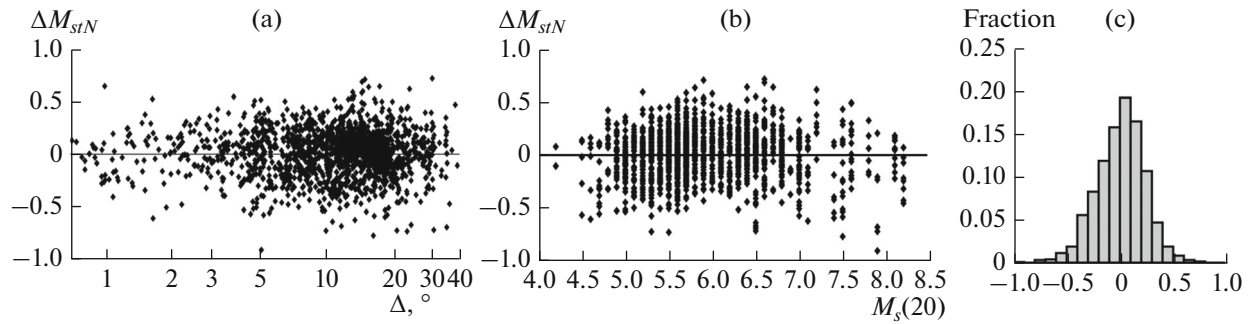


**Fig. 7.** The residuals of the station magnitude estimates  $\Delta M_{stN} = M_s(20R)_{st} - M_s(20)_{NEIC}$  by the corresponding versions of the calibration curve. The data of the three components of the record were averaged by calculating the rms value; (a), residuals  $\Delta M_{stN}$  as a function of the epicentral distance; (b), residuals  $\Delta M_{stN}$  as a function of the magnitude  $M_s(20)$ ; (c), the normalized histogram of the residuals. The estimates of the parameters of the distribution are following: mean 0.01, standard deviation 0.22.

$\Delta M_{RN}$ . The statistics of the network average magnitudes only includes the earthquakes that were recorded by at least two seismic stations. The obtained results are presented in Table 3 for the network overall and for the island-arc and continental groups of stations separately.

The figures in Tables 2 and 3 show that the developed magnitude scale is free of significant internal distortions and the accuracy of the estimates obtained based on this scale can be considered acceptable.

#### THE STATION CORRECTION FOR THE PETROPAVLOVSK SEISMIC STATION

The Petropavlovsk seismic station (PET) is the reference station in the tsunami warning service in Russia's Far East. Its properties in the context of magnitude calibration were studied more thoroughly. The

analysis revealed unexpected peculiarity which deserves discussion.

We analyzed the residuals  $\Delta M_{st}$  for the PET station:  $\Delta M_{PET} = M_s(20R)_{PET} - M_s(20R)_R$ . The results are shown in Fig. 8.

The standard deviation of the residuals  $\Delta M_{PET}$  is at most 0.16 for all the intervals of the distances. The median of the residuals' distribution for all the distances from  $0.7^\circ$  to  $40^\circ$  is below 0.003. However, the residual noticeably depends on the epicentral distance  $\Delta$ . At  $\Delta < 7^\circ$  the mean residual was  $-0.11$ , whereas at  $\Delta \geq 7^\circ$ , over an appreciably larger data, the mean residual is  $+0.02$ . The similar analysis was also conducted for the residuals  $\Delta M_{stN}$  of the PET station relative to the magnitude  $M_s(20)_{NEIC}$ . We obtained close results: at  $\Delta < 7^\circ$ , the mean is  $-0.11$ , and at  $\Delta \geq 7^\circ$ , the corresponding mean is  $+0.04$ .

Hence, this result should be regarded as objective. In the real-time analysis of the data from a single PET

**Table 2.** The parameters of the distribution of station residuals  $\Delta M_{st}$

Seismic station	Number of events	Standard deviation	Mean	Median
Island-arc stations				
PET	295	0.20	-0.01	0.01
YSS	271	0.25	0.02	0.04
MA2	59	0.23	0.06	0.06
ADK	77	0.18	-0.01	0.00
ERM	144	0.26	0.07	0.06
INCN	145	0.20	0.05	0.08
MAJO	250	0.21	-0.07	-0.05
MDJ	175	0.19	0.04	0.06
Continental stations				
BILL	57	0.21	-0.01	-0.03
TIXI	46	0.24	0.01	-0.01
YAK	24	0.20	-0.03	0.04
KAM	35	0.23	-0.02	0.08

**Table 3.** The average parameters of the distribution of magnitude residuals

Station type	Number of events	Number of station data	$\Delta M_{St}^*$	$\Delta M_{StN}$		$\Delta M_{RN}$	
			$\sigma$	$\mu$	$\sigma$	$\mu$	$\sigma$
All	371	1584	0.17	0.01	0.22	0.00	0.17
Island-arc	366	1365	0.17	0.01	0.22	0.00	0.17
Continental	60	176	0.17	0.00	0.21	-0.01	0.17

$\mu$  is mean,  $\sigma$  is standard deviation, \* mean is zero automatically.

station, at  $\Delta < 7^\circ$ , it is reasonable to correct the  $M_s(20R)$  value calculated from the record by adding +0.1 in order to compensate for the revealed anomaly. In the case of generalizing the data over a network with more than three stations, this correction can be ignored.

A similar checkup was also conducted for another reference station of the tsunami service located at Yuzhno–Sakhalinsk (YSS). No significant anomalies that would matter for real-time activities were revealed. Generally, the mean residuals in excess of 0.05 were revealed for the Japanese stations MAJO and ERM, as well as for the Magadan station MA2 (Fig. 2); however, these stations are not important for

the tasks of operatively forecasting the tsunami from a close strong earthquake.

CONCLUSIONS

The new modification of the Gutenberg  $M_s$  scale denoted by  $M_s(20R)$  enables one to have the magnitude estimates at small epicentral distances that fairly well agree with the teleseismic  $M_s(20)$  scale. The new magnitude scale relies on the amplitudes of the surface waves in the narrow interval of 16–25 s around the period of 20 s for the epicentral distances ranging from  $0.7^\circ$  to  $40^\circ$  (~80–4500 km). At small distances, the new scale uses the amplitude of the inseparable wave train of the surface waves and  $S$ -waves. The working

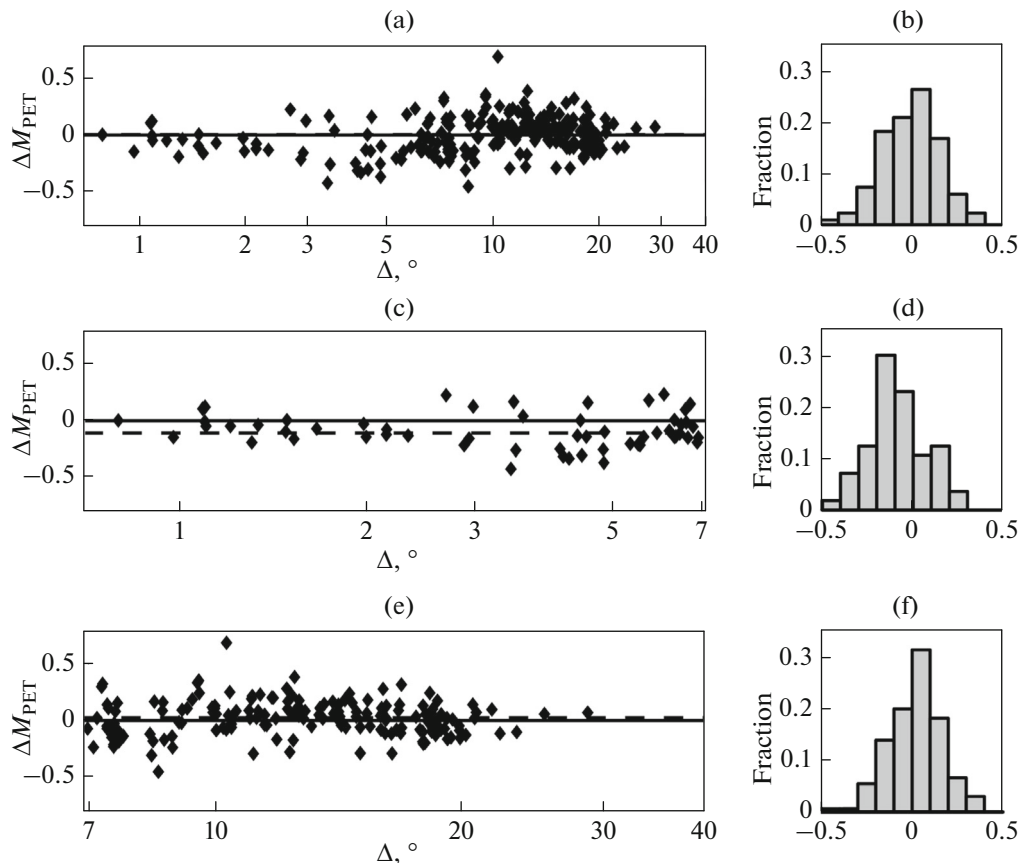


**Fig. 8.** The residuals of the estimate of magnitude  $M_s(20R)_{PET}$  determined from the PET station relative to the network-average magnitude  $M_s(20R)_R$ : (a), over the entire range of the epicentral distances; (b), the corresponding histogram; (c) and (d), the similar graphs for the short distances; (e) and (f), the similar graphs for the long distances.

interval of the periods is selected by digital filtering. The effect of digital filtering rapidly vanishes at the epicentral distances of  $\sim 20^\circ$  and longer, because the natural filtering due to the surface wave dispersion fully comes into play at these distances, which results in the automatic mutual agreement of the  $M_s(20)$  and  $M_s(20R)$  scales noted above.

The  $M_s(20R)$  magnitude scale provides the magnitude estimate at the distances of  $0.7^\circ$ – $20^\circ$ , which is convenient for picking the amplitudes and spectrally well-defined. This scale preserves historical continuity with the classical Gutenberg  $M_s$  scale. The new  $M_s(20R)$  scale for the studied region can also be used in the extended range of the epicentral distances of 2200–4500 km, where it can serve as a refinement of the standard scale  $M_s(20)$  for this distance interval. The  $M_s(20R)$  scale is suitable for making prompt estimates of magnitude, which are closely connected with the value of the seismic moment at the frequency  $1/T = 0.05$  Hz. The result will significantly improve the description of the earthquake sources in Russia's Far East. The version of the magnitude scale of 2009 has been introduced into the tsunami warning system of Russia's Far East. It was integrated into the BLITS algorithm of the automated operative data analysis (Chebrov and Gusev, 2011) and has been efficiently operating since then (Chebrov et al., 2013). The validation of the new scale for the stations of the new digital broadband seismic network in the Far East of Russia has also proven a success (V.N. Chebrov, personnel communication). Presumably the new technique for constructing the magnitude scale will also be applicable in the other regions in Russia and worldwide.

#### ACKNOWLEDGMENTS

We are grateful to S.A. Vikulina for her help in data processing, G.M. Bakhtiarova and A.Yu. Chebrova for their help in selecting the data, and M.Ya. Malkina for her technical assistance. We are grateful to the IRIS consortium for providing access to digital records.

As regards methodology, calculations and estimates (excluding data collection and measurements), the study was funded by the Russian Science Foundation (project 14-17-00621) and carried out at the Kamchatka Branch of the Geophysical Survey of the Russian Academy of Sciences.

#### REFERENCES

- Alewine, R.W., Theoretical and observed distance corrections for Rayleigh-wave magnitude, *Bull. Seismol. Soc. Am.*, 1972, vol. 62, no. 6, pp. 1611–1619.
- Bormann, P., Baumbach, M., Bock, G., Grosser, H., Choy, G.L., and Boatwright, J., Seismic source and source parameters, in *IASPEI New Manual of Seismological Observatory Practice*, Bormann, P., Ed., Potsdam: GeoForschungszentrum, 2002, vol. 1, Chapter 3, pp. 1–94.
- Bormann, P., Liu, R., Ren, X., Gutdeutsch, R., Kaiser, D., and Castello, S., Chinese national network magnitudes, their relation to NEIC magnitudes, and recommendation for new IASPEI magnitude standards, *Bull. Seismol. Soc. Am.*, 2007, vol. 97, pp. 114–127.
- Chebrov, D.V. and Gusev, A.A., Automatic real time parameter determination of tsunami earthquakes in the Far East of Russia: algorithms and software, *Seism. Instrum.*, 2011, vol. 47, no. 3, pp. 225–240.
- Chebrov, D.V., Chebrov, V.N., Vikulina, S.A., and Ototyuk, D.A., The experience of estimating the magnitudes of the strong earthquakes at the Regional Information and Processing Scientific Center (RIONTs) "Petropavlovsk" within the Tsunami warning service, in *Problemy kompleksnogo geofizicheskogo monitoringa Dal'nego Vostoka Rossii. Trudy Chetvertoi nauchno-tehnicheskoi konferentsii. Petropavlovsk-Kamchatskii* (Proc. 4th Scientific and Technical Conference on the Problems of Multiinstrumental Geophysical Monitoring of the Russian Far East), September 26–October 5, 2013, Petropavlovsk-Kamchatskii, Chebrov, V.N., Ed., Obninsk: GSRAS, 2013, pp. 299–303.
- Chubarova, O.S., Gusev, A.A., and Vikulina, S.A., The 20-second regional magnitude  $M_s(20R)$  for the Russian Far East, *Seism. Instrum.*, 2011, vol. 47, no. 3, pp. 241–245.
- Droznin, D.V. and Droznina, S.Ya., Interactive DIMAS program for processing seismic signals, *Seism. Instrum.*, 2011, vol. 47, no. 3, pp. 215–224.
- Evernden, J.F., Variation of Rayleigh-wave amplitude with distance, *Bull. Seismol. Soc. Am.*, 1971, vol. 61, pp. 231–240.
- Gutenberg, B., Amplitudes of surface waves and magnitude of shallow earthquakes, *Bull. Seismol. Soc. Am.*, 1945, vol. 35, pp. 3–12.
- Herak, M. and Herak, D., Distance dependence of  $M_s$  and calibration function for 20-second Rayleigh waves, *Bull. Seismol. Soc. Am.*, 1993, vol. 83, pp. 1881–1892.
- Marshall, P.D. and Basham, P.W., Rayleigh wave magnitude scale  $MS$ , *Pure Appl. Geophys.*, 1973, vol. 103, pp. 406–414.
- Okal, E.A., A theoretical discussion of time domain magnitudes: the Prague: formula for  $MS$  and the mantle magnitude  $M_m$ , *J. Geophys. Res.*, 1989, vol. 94, no. B4, pp. 4194–4204.
- Panza, G.F., Duda, S.J., Cernobori, L., and Herak, M., Gutenberg's surface-wave magnitude calibration function: theoretical basis from synthetic seismograms, *Tectonophysics*, 1989, vol. 166, pp. 35–43.
- Rezapour, M. and Pearce, G.P., Bias in surface-wave magnitude  $MS$  due to inadequate distance corrections, *Bull. Seismol. Soc. Am.*, 1998, vol. 88, pp. 43–61.
- von Seggern, D., Amplitude-distance relation for 20-second Rayleigh waves, *Bull. Seismol. Soc. Am.*, 1977, vol. 67, pp. 405–411.
- Singh, S.K. and Pacheco, J.F., Magnitude determination of Mexican earthquakes, *Geofis. Int.*, 1994, vol. 33, pp. 189–198.
- Solov'ev, S.L., On the regional distinctions of the calibration curve for calculating the surface wave magnitudes, in *Magnituda i energeticheskaya klassifikatsiya zemletryasenii. Sbornik statei v dvukh tomakh* (The Magnitude and Energy Classification of the Earthquakes. Collection of Papers in Two Volumes), Moscow: IFZ AN SSSR, 1974, vol. 2, pp. 55–59.
- Vanek, I., Zatopek, A., Karnik, V., Kondorskaya, N.V., Riznichenko, Yu.V., Savarenskii, E.F., Solov'ev, S.L., and Shebalin, N.V., Standard magnitude scale, *Izv. Akad. Nauk SSSR, Ser. Geofiz.*, 1962, no. 2, pp. 153–158.

Translated by M. Nazarenko